Journal of Applied Polymer Science

Physicochemical characterization of lignin recovered from microwave-assisted delignified lignocellulosic biomass for use in biobased materials

Jiulong Xie,[1,2] Chung-Yun Hse,[3] Todd F. Shupe,[2] Tingxing Hu[1]

[1]Department of Wood Science, College of Forestry, Sichuan Agricultural University, Chengdu, Sichuan 611130, China

[2]Louisiana Forest Products Development Center, School of Renewable Natural Resource, Louisiana State University Agricultural Center, Baton Rouge, Louisiana 70803

[3]Southern Research Station, USDA Forest Service, Pineville, Louisiana 71360

Correspondence to: T. Hu (E-mail: tingxing_hu@163.com)

ABSTRACT: Lignocellulosic biomass (Moso Bamboo, Chinese tallow tree wood, switchgrass, and pine wood) was subjected to a novel delignification process using microwave energy in a binary glycerol/methanol solvent. The physicochemical properties of the recovered lignin were analyzed prior to its application in the fabrication of polylactic acid (PLA)–lignin composites. The results showed that the samples had a high Klason lignin content (>75%) and retained their natural structure. Thermogravimetric analysis revealed that the recovered lignin exhibited a different thermal decomposition pattern from that of commercial lignins. All the recovered lignins had good solubility in common organic solvents (acetone, 1,4-dioxane, THF, DMSO, and ethanol/water) and 1 mol/L NaOH solution. The addition of lignin into the PLA matrix resulted in the improvement in tensile properties of PLA–lignin composites. PLA films with low lignin content had good UV light-resistant properties, indicating that the recovered lignin has potential in packaging of light-sensitive products. © 2015 Wiley Periodicals, Inc. J. Appl. Polym. Sci. **2015**, *132*, 42635.

KEYWORDS: lignocellulosic biomass; lignin; microwave delignification; poly lactic acid

Received 27 April 2015; accepted 17 June 2015

DOI: 10.1002/app.42635

INTRODUCTION

Alcohol-based such as bioethanol derived from biomass have attracted the attention of researchers worldwide because of the continuing depletion of fossil fuels. However, to facilitate large-scale utilization, it is imperative to develop an economic and cost-effective process for commercial implementation of biofuels.[1] Lignocellulosic biomass, primarily composed of cellulose, hemicellulose, and lignin, has been considered the most suitable for biofuels and green chemical production. Therefore, the use of substrates such as lignocellulosic biomass in the form of agricultural and forest residues is a viable solution to boost the economic viability of biofuels. However, the most costly component of alcoholic biofuel synthesis is the pretreatment of the biomass prior to fermentation. The maximum amount of sugar monomers (mainly cellulose and hemicellulose) from raw biomass is necessary for efficient and economic alcoholic biofuel production.[2] Lignin, which fills the space between cellulose and hemicelluloses and crosslinks with hemicellulosic polysaccharides, acts as a barrier for the accessibility of chemicals and enzymes to cellulose.[3] It is, therefore, necessary to extract lignin. Various pretreatment processes of lignocellulosic biomass, such as acidic/alkaline pretreatment,[4] wet oxidative,[5] steam explosion,[6] ultrasound-assisted,[7] and mechanical forces,[8] have been applied in the fractionation of different lignocellulosic biomass to fulfill the demand for lignocellulosic bioethanol.

However, lignin from the biorefinery industries is currently an underutilized waste product because lignin is often relegated to the low value of combustion or sold as a natural component for animal feeds.[9] About 225 million tons of lignin generation is expected from the cellulosic alcohol industry in the United States in the near future, and only 2% is being used for value-added applications.[10] Therefore, new processes are needed that generate value-added products from lignin to sustain the lignocellulosic bioethanol industry. Several studies have explored the use of lignin as an inexpensive filler/additive component to modify thermoplastic material properties such as hydrophobicity, stiffness, and mechanical properties.[11–17] Liquefied/depolymerized lignin usually with high reactivity and low molecular weight has been applied in the fractionation of green polyurethane foams and other biobased products.[18,19] With all these attempts to expand the industrial applications of lignin in

thermoplastic industries, polylactic acid (PLA) is mainly used as the plastic matrix because of its biodegradable character. In addition, PLA also plays a predominant role as a sustainable alternative to petrochemical-derived products. Recently, PLA has been widely studied for use in packaging materials.[20,21] However, the use of PLA in the packaging industry is limited to the production of high-valued products such as films and rigid thermoforms because of its high cost.

In our recent studies, lignin samples were recovered from a microwave-assisted delignification system. The objective of this study is to understand the recovered lignin fraction and its potential applications in biobased materials. Therefore, the physicochemical characteristics of the lignins were evaluated. PLA–lignin composites were prepared, and the mechanical properties, thermal stability, and optical transmission of the obtained materials were determined. The results of this study will provide preliminary information to facilitate the commercialization of lignin byproducts from biorefinery industries.

EXPERIMENTAL

Materials and Chemicals

Moso bamboo, Chinese tallow tree wood, pine wood, and switchgrass were chosen as the experimental feedstocks. All materials were harvested from the Kisatchie National Forest, Pineville, Louisiana, USA. Each sample was reduced to particles using a Thomas Wiley Laboratory mill. The particles were screened to collect particles that passed through a 20-mesh sieve and then retained on a 40-mesh sieve and then dried to a constant weight in an oven maintained at 80°C. The dried particles were stored in polyethylene bags and used without further treatment. The density and melt flow index of the PLA matrix was 1.24 g/cm^3 and 20 g/10 min at 190°C/2.16 kg, respectively. All chloroform, glycerol, methanol, and acid used were of reagent grade and obtained from commercial sources. Westvaco and Reed lignins were purchased and used as industrial lignin samples.

Microwave-Assisted Delignification and Lignin Recovery

Delignification of lignocellulosic biomass was carried out in a Milestone MEGA laboratory microwave oven at an output power of 550 W using a modified solvolysis liquefaction process. Mixture of glycerol and methanol [glycerol/methanol: 2/1 (w/w)] was used as the solvent, and sulfuric acid was used as the catalyst. A typical reaction mixture consisting of 2 g of lignocellulosic particles, 8 g of solvent, and 0.14 g of sulfuric acid was loaded in Teflon vessels with a magnetic stirring bar. The Teflon vessels were then placed on a rotor tray inside the microwave cavity. The temperature was monitored using an ATC-400FO automatic fiber optic temperature control system. Based on the monitored temperature, the output power was autoadjusted during liquefaction. In this study, the temperature was increased from room temperature to 120°C at a heating rate of 25°C/min and was then kept constant for 4 min. After a cooling period of 30 min at the end of reaction, the resulting reaction mixtures were then vacuum-filtered through Whatman No. 4 filter paper.

The filtrated liquid was evaporated at 45°C under vacuum to remove methanol, and then distilled water [10/1 (w/w)] was added to the obtained liquid. The mixture was stirred thoroughly with a glass rod. Afterward, the mixture was centrifuged at 5000 rpm for 10 min. The precipitates were dried at 30°C for 12 h. The recovery yield is the mass percentage of the precipitates to the original weight of lignocellulosic biomass.

Preparation of PLA–Lignin Composites

PLA and lignin samples were vacuum-dried at 60°C for 24 h before the preparation of PLA–lignin composites. Recovered bamboo lignin samples (25 mg) were stirred in 5 mL of 1,4-dioxane for 20 min. Thereafter, the lignin solution was blended with PLA (500 mg) in 10 mL chloroform for 2 h. Then, the mixture was vacuum-dried at 60°C prior to use. PLA–lignin composites were prepared by a hot-press (Carver Laboratory Press, Model C) process. The dried mixture was first kept at 180°C for 20 s without pressure, then 0.125 ton for 15 s, and then 0.5 ton for 90 s.

Wet Chemistry Analysis

The Klason lignin and ash content of the samples was determined according to the ASTM standards D-1105-96 and D-1102-84, respectively.[22,23]

FTIR Spectra

The FTIR analysis was performed by a Nicolet Nexus 670 spectrometer equipped with a Thermo Nicolet Golden Gate MKII Single-Reflection ATR accessory. Data collection was performed with a 4 cm^{-1} spectral resolution, and 32 scans were taken per sample.

Thermogravimetric Analysis

Thermogravimetric analysis (TGA)/differential thermogravimetric (DTG) analysis was conducted with a thermal analyzer, TGA (Q50), to simultaneously obtain thermogravimetric data. About 2 mg of sample was analyzed by the thermal analyzer. Pyrolysis was terminated at 800°C with a heating rate of 20°C/min under a flow of 60 mL/min of nitrogen gas.

Mechanical Testing

The mechanical properties of PLA–lignin composites were characterized by the tensile strength, and the specimen used for the experiments was sample strips of 50 mm × 5 mm × 0.1 mm. The tensile tests were performed using an Instron testing machine (Instron 4465), with a load of 5 kN at a crosshead speed of 5 mm/min. Five replicates for each type of composite were tested, and the average values are presented.

Optical Transmittance

The transmittance of neat PLA and PLA–lignin films 0.03 mm in thickness was measured using an HP UV–vis spectrometer (UV-HP 8453). The samples were scanned from 190 to 800 nm.

RESULTS AND DISCUSSION

Recovery Yield

The recovery lignin yield and its main composition were determined and presented in Table I. The recovery lignin yield was 17.62, 23.04, 20.78, and 18.75% for bamboo, Chinese tallow tree wood, switchgrass, and pine wood, respectively, whereas the original Klason lignin content in bamboo, Chinese tallow tree wood, switchgrass, and pine wood was 20.91, 19.13, 20.61, and 30.96%, respectively. No significant difference in the lignin recovery yield and the original Klason lignin content was found

Table I. Recovery Yield and Main Component of the Lignin Samples

Biomass type	Recovery yield (%)	Klason lignin (%)	Ash content (%)
Bamboo	17.62	75.66	0.031
Chinese Tallow tree	23.04	75.63	0.057
Switchgrass	20.78	77.56	0.091
Pine wood	18.75	75.44	0.010

except for pine wood. All the recovered lignin samples showed high Klason lignin content (>75%). Recovered lignin samples except switchgrass had low ash content (0.01–0.06%).

Chemical Structure

The FTIR analysis was used for in-depth elucidation of structural features of the recovered lignin, and the IR spectra of the recovered lignin as well as industrial lignin sample (Westvaco lignin) are depicted in Figure 1. The assignments of absorption bands corresponding to different functional groups of lignin are presented in Table II.[24,25] The bands at around 3389 cm^{-1} are assigned to O—H stretching and were weak bands in all the lignin samples. The bands at around 2938 and 2847 cm^{-1} are assigned to CH stretch in CH_2 and CH_3 groups. Typical lignin absorption bands, such as aromatic ring vibration of phenyl-propane (1601–1594 cm^{-1}), aromatic ring vibration C=C of the benzene ring (1506–1501 cm^{-1}), and C—H deformation combined with aromatic ring vibration (1459–1451 cm^{-1}), were significantly visible in all lignin spectra. This confirmed that the core structure of the lignin was still retained after the delignification process.

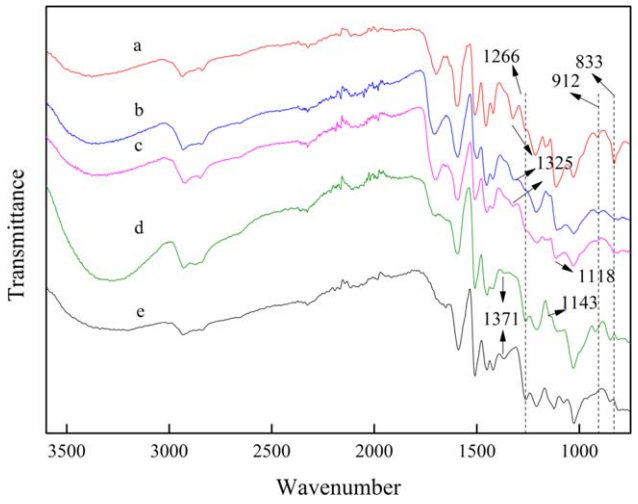

Figure 1. FTIR spectra of lignin samples recovered from delignified (a) bamboo, (b) Chinese tallow tree, (c) switchgrass, (d) pine wood, and (e) Westvaco lignin. [Color figure can be viewed in the online issue, which is available at wileyonlinelibrary.com.]

However, significant differences in bands attributed to lignin functional groups were also observed among lignin samples recovered from different lignocellulosic biomass types. The bands at 1371 cm^{-1}, which is assigned to O—H deformation in phenols, were apparent in the spectra of the Westvaco lignin and lignin recovered from pine wood, whereas they were almost invisible in the lignin spectra of bamboo, Chinese tallow tree wood, and switchgrass. Lignin structure bands at 1325 cm^{-1} assigned to S-ring breathing and G-ring substituted in position 5 and 1116–1113 cm^{-1} assigned to aromatic C—H in-plane deformations (S units) were found in the lignin spectra of bamboo, Chinese tallow tree wood, and switchgrass; however, the

Table II. Band Assignments in FTIR

Wavenumber (cm^{-1})	Assignment
3330-3389	O—H stretching (rupture of cellulose hydrogen bonds)
2926-2938/2834-2847	C—H stretch in methyl and methylene groups
1741-1719	Cz=O stretching due to ester linkage between carbohydrate and lignin
1601-1594	Aromatic ring vibration of phenyl-propane (C_9)
1506-1501	Aromatic skeletal vibration C=C of the benzene ring
1458-1451	C—H deformation combined with aromatic ring vibration
1430-1419	Aromatic skeletal vibrations associated with C—H in plane deformation in cellulose
1371	Aliphatic C—H symmetric deformation in methyl
	+ O—H deformation in phenols
1320-1326	S-ring breathing + G-ring substituted in position 5
1266-1272	G-ring breathing and C—O stretching
1213-1218	C—O stretching in phenols and ethers
1114/1143	Aromatic C—H in-plane deformations (S units)
1026-1030	Aromatic C—H in-plane deformations in G units
	+ C—O deformations in primary alcohols
909-918	Aromatic C—H out-of-plane deformation (only in GS lignin type)
830/809	Aromatic C—H out-of-plane in position 2 and 6 from S unit

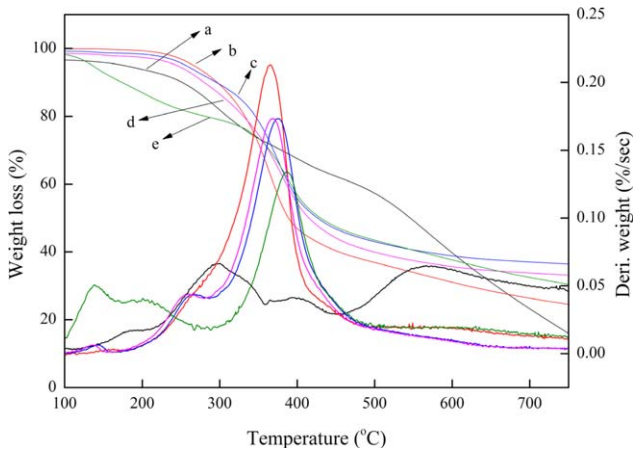

Figure 2. TG and DTG curves of (a) Westvaco lignin and recovered (b) bamboo lignin, (c) Chinese tallow tree lignin, (d) switchgrass lignin, and (e) pine wood lignin. [Color figure can be viewed in the online issue, which is available at wileyonlinelibrary.com.]

former band was absent and the latter shifted to 1143 cm^{-1} in the lignin spectra of pine wood and Westvaco. Such shifts of this band toward to higher wavenumbers usually contributed to the increase in S units.[26] Meanwhile, bands at 912 and 833 cm^{-1} contributed to aromatic C—H out-of-plane deformation, specific to hardwood lignin, were also absent in the lignin spectra of pine wood and Westvaco. C—O stretching in G lignins appeared at bands of 1266 cm^{-1} in the pine wood lignin spectrum, which confirmed that pine wood possessed high fraction of G units.

By comparing the spectra between pine wood and Westvaco lignin, it was found that the two spectra were almost identical, suggesting that the structures of the recovered pine wood lignin were close to that of Westvaco lignin. The FTIR results clearly showed that Chinese tallow tree wood and pine wood lignins still contain traces of hardwood and softwood lignin functional groups, respectively.

Thermal Behavior

TGA and DTG analysis of recovered lignin samples from different lignocellulosic biomass are described in Figure 2. Thermal decomposition profiles of commercially obtained lignin sample (Westvaco lignin) were also tested as a comparison. As shown in Figure 2, the Westvaco lignin was thermally decomposed over a wide temperature (130–800°C) with two maximum decomposition rates. Accordingly, the lignin structure is very complex because it is mainly composed of aromatic rings with C_α-C_β-C_γ side chains and has various oxygen functional groups.[27] These structural characteristics result in an extremely wide temperature range of decomposition. Two thermal events were identified during the degradation of the Westvaco lignin: in the first step (240–420°C), volatiles such as CO_2, H_2O, and CO were primarily released by breaking the side chains of carboxyl groups, hydroxyl groups, and aldehyde groups, respectively; and in the second one (450–800°C), the primarily released substances were CH_4 (generated by breaking the methoxy group OCH_3—), CO_2, and CO.[26] The DTG curves of Westvaco lignin showed wide and flat peaks with a gently sloping baseline. This is different for the sharp DTG peaks of recovered lignins with a flat tailing section at higher temperatures. It was evident that the structural groups of the recovered lignin differed significantly from the Westvaco lignin.

Variability in the weight loss occurred at the initial stages (180–300°C), which was mainly due to the decomposition of side chains connected to the multiple interunits, were found among different recovered lignin samples. For the decomposition of recovered pine wood lignin, it started at relative low temperature (180°C) with a flat peak, whereas decomposition of the Chinese tallow tree wood and switchgrass lignin samples occurred at 230–280°C, with small peaks at 249 and 274°C, respectively. The result indicated that more substances with lower molecular weight in pine wood lignin were degraded during this decomposition stage. This may be explained by the results of FTIR analysis, as discussed above. The breaking of hydroxyl groups specific to pine wood lignin that were indicated by the band at 1371 cm^{-1} released more H_2O, which resulted in a larger initial weight loss at relative low temperature. Interestingly, no apparent weight loss was observed at this stage for recovered bamboo lignin. This may be due to the absence or few of side-chain groups in recovered bamboo lignins.

By comparing the maximum decomposition rate temperature (T_{max}) as observed in the TGA curves among the recovered lignin samples, it was found that the pine wood lignin had higher T_{max} than that for the other three lignins, indicating that the recovered pine wood lignin was thermally stable. This finding was in good agreement with the result that the coniferous lignin was more thermally stable than deciduous lignin because T_{max} for pine wood lignin obtained in this study was about 10°C higher than that for Chinese tallow tree wood lignin.[28] This result also clarified that lignin recovered from the microwave-assisted delignification process retained their natural origin structure, which is consistent with the FTIR analysis results.

Solubility

The insolubility of the pulping industrial lignins in common solvents has severely inhibited efforts to produce value-added platform chemicals because of their poor molecular interactions with other reagents. To evaluate the solubility of the recovered lignins, samples were tested in several organic solvents [acetone, ethanol/water (7/3), THF, DMSO, and 1,4-dioxane]. The results showed that all the recovered lignin samples were completely soluble in acetone, ethanol/water, THF, DMSO, and 1,4-dioxane at an initial test concentration of 1 mg/mL. In addition, the recovered lignins were completely soluble in 1 mol/L solution of NaOH. For comparative purpose, the solubility of recovered bamboo lignin and two commercial lignin samples (Westvaco and Reed lignin) were further tested. As shown in Figure 3, by adding lignin in the solvents to 5 mg/mL, the bamboo lignin could be completely soluble, whereas the Westvaco lignin was partially soluble and the Reed lignin was completely insoluble. These results suggested that the recovered lignin should have better reaction activity because a homogeneous phase can be formed in many reactions by solvents.

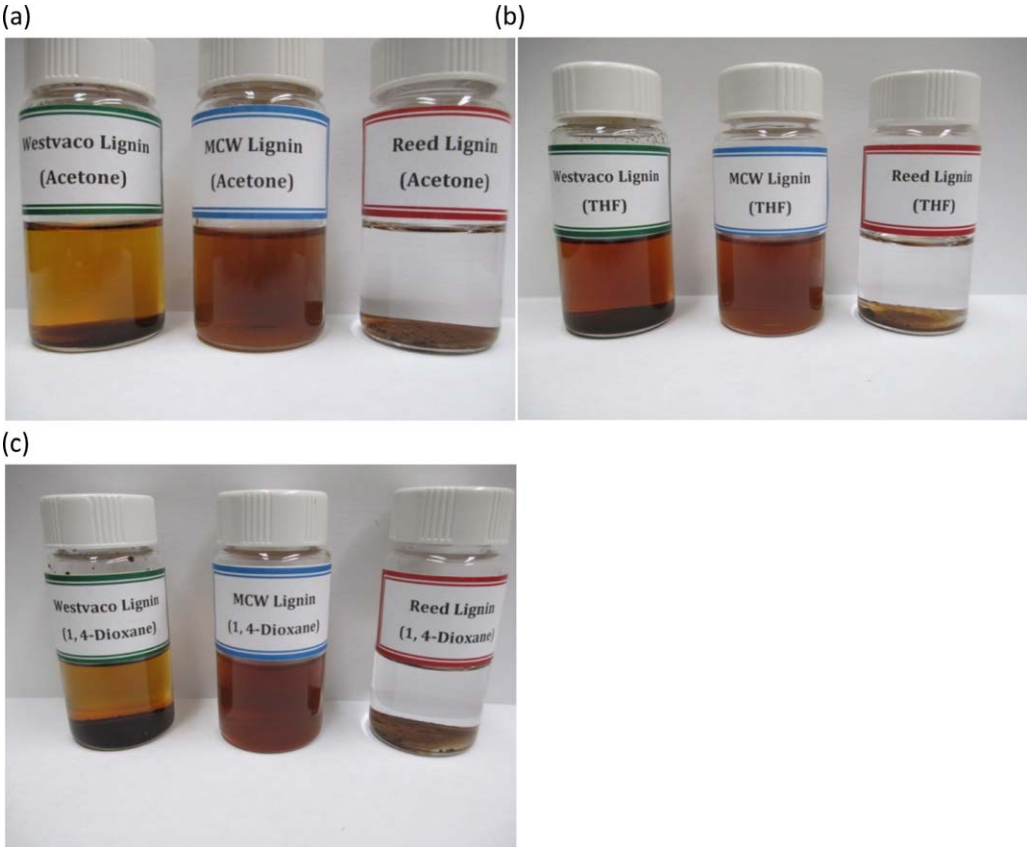

Figure 3. Photograph of bamboo lignin in (a) acetone, (b) THF, and (c) 1,4-dioxane. MCW lignin: Bamboo lignin samples obtained in this study. [Color figure can be viewed in the online issue, which is available at wileyonlinelibrary.com.]

Preparation and Characteristics of PLA–Lignin Composites

Neat PLA composite and PLA–lignin composites with different lignin contents (1, 5, and 10 wt %) were prepared, and the tensile properties are reported in Table III. The tensile strength, tensile modulus, and strain of the neat PLA composite were 40.38 ± 6.64 MPa, 2.56 ± 0.30 GPa, and $2.58 \pm 0.49\%$, respectively. The addition of lignin into PLA contributed to increase in tensile properties. With 1 wt % of lignin, the increments in tensile properties for the composites are 32.17, 12.89, and 10.07% for tensile strength, tensile modulus, and strain, respectively. Similar results were obtained by Chung *et al.*,[16] who reported that the incorporation of modified lignin-*g*-PLA copolymers into PLA could result in a modest increase in tensile strength and strain, whereas the unmodified lignin addition decreased the tensile strength. Other studies argued that the addition of commercial lignin to polymer matrix decreased the mechanical properties of composites, whereas the addition of acetylated commercial lignin or organosolv lignin contributed to improved mechanical properties.[15,17] Surface modification, mainly via acetylation of lignocellulosic components (cellulose fibers or lignin), could increase their dispersion and affinity with biopolymers, and the good interfacial adhesion between the modified lignocellulosic components and polymer matrix attributed to the higher mechanical properties of biobased materials.[15,29] Based on these results, it can be easily understood that the higher tensile properties of PLA–lignin composites obtained in this experiment when compared with neat PLA composites is due to the well dispersion of lignin and its interfacial adhesion with PLA because of its good solubility as discussed above.

TG and DTG curves of neat PLA and PLA–lignin composites are shown in Figure 4. The initial decomposition temperature corresponding to 5% weight loss ($T_{5\%}$), maximum degradation rate temperature (T_{max}), and char yield are presented in Table

Table III. Mechanical Properties of PLA–Lignin Composites

Composition	Tensile strength (MPa)	Tensile strain (%)	Tensile modulus (GPa)
PLA	40.38 ± 6.64	2.56 ± 0.30	2.58 ± 0.49
PLA/1% lignin	53.37 ± 7.84	2.89 ± 0.38	2.84 ± 0.59
PLA/5% lignin	48.38 ± 8.92	2.81 ± 0.73	3.04 ± 0.29
PLA/10% lignin	49.59 ± 6.55	2.50 ± 0.43	3.16 ± 0.03

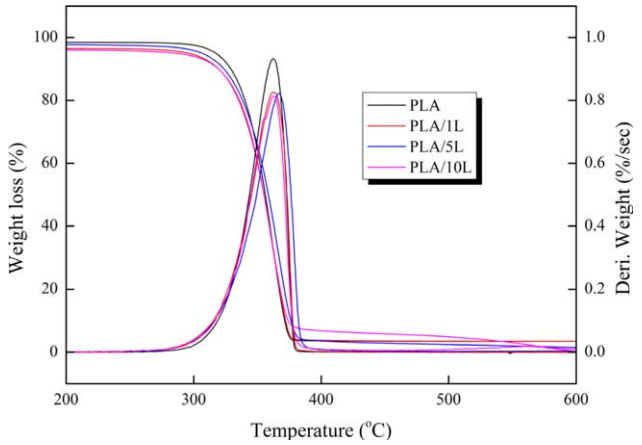

Figure 4. TG and DTG curves of neat PLA composites (PLA) and PLA–lignin composites (PLA/1L, PLA/5L, and PLA/10L for composites with 1, 5, and 10% bamboo lignin content, respectively). [Color figure can be viewed in the online issue, which is available at wileyonlinelibrary.com.]

IV. The $T_{5\%}$ of the neat PLA composite was particularly high in comparison with PLA–lignin composites. This is mainly due to the decomposition of lignin substances with low molecular weight as the decomposition of lignin started at low temperature (180–300°C) and covered a wide temperature range as discussed above. T_{max} for the PLA–lignin composites are a little bit higher than that for the neat PLA composite; however, no significant difference was found. It was reported that the good compatibility of lignin with a PLA matrix resulted in a good retention of the thermal properties.[11] From this point of view, the good miscibility of the recovered lignin with PLA is the reason that the T_{max} is not obviously affected by the addition of lignin. Char yield showed a decrease with the addition of lignin, which was contrasted with the results in another study.[14] This result may be due to the character differences among various lignin sources.

The transmissions of visible and ultraviolet light are important parameters in designing the right packaging materials to preserve and protect light-sensitive foods/products. Despite the fact that PLA films had better UV light barrier properties than LDPE, it is slightly worse than those of PET which does not transmit both UV-C (100–280 nm) and UV-B (280–315 nm).[30] As shown in Figure 5, PLA showed no UV light transmission in the lower range of UV-C (100–230 nm), whereas the UV light is transmitted in the higher range of UV-C (230–280 nm) and nearly all the UV-B (280–315 nm) and UV-A (315–400 nm) light passed through the PLA films. The addition of a small amount of the recovered lignin (0.5 wt %) in PLA resulted in an significant improvement in light barrier properties, that is, about 80% of UV-C (230–280 nm) and 40% of UV-B light (280–315 nm) were blocked by the PLA–lignin films. By adding 1 wt % of lignin in PLA, the PLA–lignin film blocked nearly all the UV-C and UV-B and 75–80% of UV-A light. The result revealed that the recovered lignin could be used as an efficient additive in PLA to block UV light transmission.

Table IV. Temperature and Char Residue Characteristics of PLA–Lignin Composites

Sample	$T_{5\%}$ (°C)	T_{max} (°C)	Char yield (%)
PLA	317.15	361.78	3.42
PLA-1% lignin	295.57	362.39	3.46
PLA-5% lignin	306.45	362.65	0.07
PLA-10% lignin	286.04	366.89	1.04

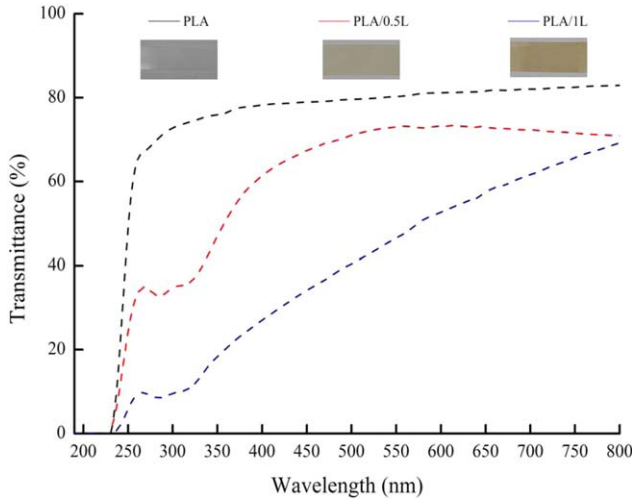

Figure 5. UV–vis spectra of PLA and PLA–lignin composites (PLA/0.5L and PLA/1L for composite with 0.5 and 1% bamboo lignin content, respectively). [Color figure can be viewed in the online issue, which is available at wileyonlinelibrary.com.]

CONCLUSIONS

Lignins recovered from microwave-assisted delignified lignocellulosic biomass system showed high purity and retained their natural structures. Lignin samples from delignified pine wood exhibited the highest thermal stability. All the lignin samples could be completely soluble in ethanol/water, DMSO, THF, 1,4-dioxane, and 1 mol/L NaOH solution. The PLA–lignin composites had higher tensile properties than that for neat PLA composite. The addition of lignin into PLA had no significant influence on the thermal degradation property of the composites. Lignin component in the PLA–lignin blends significantly improved the UV light barrier properties of the composites.

REFERENCES

1. Shrotri, A.; Lambert, L. K.; Tanksale, A.; Beltramini, J. *Green Chem.* **2013**, *15*, 2761.
2. Singh, S.; Bharadwaja, S. T. P.; Yadav, P. K.; Moholkar, V. S.; Goyal, A. *Ind. Eng. Chem. Res.* **2014**, *53*, 14241.
3. Saha, B. C.; Cotta, M. A. *J. Chem. Technol. Biotechnol.* **2007**, *82*, 913.
4. Zhou, S.; Liu, L.; Wang, B.; Xu, F.; Sun, R. C. *Process Biochem.* **2012**, *47*, 1799.
5. Lissens, G.; Klinke, H.; Verstraete, W.; Ahring, B.; Thomsen, A. B. *J. Chem. Technol. Biotechnol.* **2004**, *79*, 889.

6. Sun, F. B.; Chen, H. Z. *J. Chem. Technol. Biotechnol.* **2008**, *83*, 707.
7. Subhedar, P. B.; Gogate, P. R. *Ultrason. Sonochem.* **2014**, *21*, 216.
8. Stein, T. V.; Grande, P. M.; Kayser, H.; Sibilla, F.; Leitner, W.; Maria, P. D. *Green Chem.* **2011**, *3*, 1.
9. Holladay, J. E.; Bozell, J. J.; White, J. F.; Johnson, D. Top Value-Added Chemicals from Biomass. Volume II Results of Screening for Potential Candidates from Biorefinery Lignin. Pacific Northwest National Laboratory: Richland, WA, **2007**.
10. Satheesh, K. M. N.; Mohanty, A. K.; Erickson, L.; Misra, M. *J. Biobased Mater. Bioeng.* **2009**, *3*, 1.
11. Li, J. C.; He, Y.; Inoue, Y. *Polym. Int.* **2003**, *52*, 949.
12. Yang, Y.; Deng, Y. H.; Tong, Z.; Wang, C. Y. *ACS Sustain. Chem. Eng.* **2014**, *2*, 1729.
13. Sahoo, S.; Misra, M.; Mohanty, A. K. *Compos. A* **2011**, *42*, 1710.
14. Ouyang, W. Z.; Huang, Y.; Luo, H. J.; Wang, D. S. *J. Polym. Environ.* **2012**, *20*, 1.
15. Gordobil, O.; Egues, I.; Liano-Ponte, R.; Labidi, J. *Polym. Degrad. Stab.* **2014**, *108*, 330.
16. Chung, Y. L.; Olsson, J. V.; Li, R. J.; Frank, C. W. *ACS Sustain. Chem. Eng.* **2013**, *1*, 1231.
17. Spiridon, I.; Leluk, K.; Resmerita, A. M.; Darie, R. N. *Compos. B* **2015**, *69*, 342.
18. Cinelli, P.; Anguillesi, I.; Lazzeri, A. *Eur. Polym. J.* **2013**, *49*, 1174.
19. Xue, B. L.; Wen, J. L.; Sun, R. C. *Materials* **2015**, *8*, 586.
20. Arrieta, M.; Lopez, J.; Hernandez, A.; Rayon, E. *Eur. Polym. J.* **2014**, *50*, 255.
21. Tawakkal, I.; Cran, M. J.; Miltz, J.; Bigger, S. W. *J. Food Sci.* **2014**, *79*, R1477.
22. American Society for Testing and Materials (ASTM). Standard Test Method for Acid-Insoluble Lignin in Wood. ASTM D-1105-96. American Society for Testing and Materials: Philadeliphia, U.S.A. **1996**.
23. American Society for Testing and Materials (ASTM). Standard Test Method for Ash in Wood. ASTM D-1102-84. American Society for Testing and Materials: Philadeliphia, U.S.A. **1990**.
24. Garmakhany, A. D.; Kashaninejad, M.; Aalami, M.; Maghsoudlou, Y.; Khomieri, M.; Tabil, L. G. *J. Sci. Food Agric.* **2014**, *94*, 1607.
25. Gabov, K.; Gosselink, R. J. A.; Smeds, A. I.; Fardim, P. *J. Agric. Food Chem.* **2014**, *62*, 10759.
26. Brebu, M.; Vasile, C. *Cell. Chem. Technol.* **2009**, *44*, 353.
27. Kim, J. Y.; Hwang, H.; Oh, S.; Kim, Y. S.; Kim, U. J.; Choi, J. W. *Int. J. Biol. Macromol.* **2014**, *66*, 57.
28. Muller-Hagedorn, M.; Bockhorn, H.; Krebs, L.; Muller, U. *J. Anal. Appl. Pyrolysis* **2003**, *68/69*, 231.
29. Abdulkhani, A.; Hosseinzadeh, J.; Ashori, A.; Dadashi, S.; Takzare, Z. *Polym. Test.* **2014**, *35*, 73.
30. Auras, R.; Harte, B.; Selke, S. *Macromol. Biosci.* **2004**, *4*, 835.